Original Article

Integration accuracy of craniofacial cone-beam computed tomography images with three-dimensional facial scans according to different registration areas

Hussein Aljawad[a]; Nara Kang[b]; Kyungmin Clara Lee[c]

ABSTRACT

Objectives: To evaluate the integration accuracy of cone-beam computed tomography (CBCT) images with three-dimensional (3D) facial scans according to different registration areas.

Materials and Methods: Twenty-five patients (14 males and 11 females), with a mean age of 19.0 ± 11.3 years, were included in this study. Each patient underwent CBCT and facial scans on the same day in an upright position. The facial scans were integrated with the corresponding soft-tissue images of CBCT scans. Three methods were used to integrate the two imaging modalities based on the facial regions scanned: R1, only the forehead and nasal bridge area were included; R2, the right and left malar area were included; and R3, the forehead, nasal bridge, and malar areas were included. The integration accuracy between the facial scans and CBCT images was evaluated by color-mapping methods and average surface distances, calculated by measuring the 3D distances between the surface points on the two superimposed images.

Results: The average surface differences between facial scans and CBCT images were less than 1.0 mm in all three methods. The R3 method showed fewer differences between the facial scans and CBCT images than the other methods did.

Conclusions: Facial scans obtained using a low-cost facial scanner showed clinically acceptable performance. The integration accuracy of facial and CBCT scans can be increased by including the forehead, nasal bridge, and malar areas as registration areas. (*Angle Orthod.* 2022;93:66–70.)

KEY WORDS: Integration; Registration; CBCT; Facial scan

INTRODUCTION

Three-dimensional (3D) facial scanners are becoming an increasingly essential tool for the analysis of facial asymmetry as well as for monitoring patients undergoing maxillofacial surgery. Because of the lack of true color and surface texture on cone-beam computed tomography (CBCT) images, the integration of 3D facial scans with CBCT images has become an important method for assessing craniomaxillofacial surgical and nonsurgical treatments.[1–3]

With recent technological advancements, various facial scanners have been introduced with different technologies and advantages. Stereophotogrammetry is the most common type of 3D surface imaging system technology.[4] Because of its fast capture speed and ease of use, 3D stereophotogrammetry can be used for 3D facial evaluation of patients following craniomaxillofacial surgery. However, stereophotogrammetry scanners have the drawback of a large footprint, high cost, and the need for meticulous calibration, which make them unsuitable for daily clinical practice.[5]

Structured-light 3D scanners use projected light patterns and a camera system.[6] Previous studies have shown that structured light scanners have high accuracy but require a long scanning time because of inadequate coverage of the scanned object, namely, the concave and convex areas of the face, such as the nose, make the scanning time longer.[6,7] In addition, as

[a] Postgraduate student, Department of Orthodontics, School of Dentistry, Chonnam National University, Gwangju, Korea.

[b] Private practice, Department of Oral and Maxillofacial Surgery, Division of Jaw Surgery and Sleep Surgery, Sun Dental Hospital, DaeJeon, Korea.

[c] Professor, Department of Orthodontics, School of Dentistry, Chonnam National University, Gwangju, Korea.

Corresponding author: Kyungmin Clara Lee, Department of Orthodontics, School of Dentistry, Chonnam National University, 33 Yongbong-ro, Buk-gu, Gwangju 61186, Korea
(e-mail: ortholkm@jnu.ac.kr)

Accepted: June 2022. Submitted: February 2022.
Published Online: July 27, 2022

with all optical methods, reflective or transparent surfaces cause difficulties. To overcome these disadvantages of 3D facial scanners, a photo-wrapping technique that uses facial photos and CBCT scans has been suggested.[8,9] However, some anatomical structures such as the subnasal areas might be hidden behind the shadow of other structures.

Recently, various low-cost facial scanners have been introduced. They offer advantages such as lower cost, quicker scan time, easy application to daily clinical practice, and no requirement for extensive calibration. Currently, 3D facial scans are currently used only as an additional tool and are not used independently for diagnosis and treatment evaluation in patients undergoing maxillofacial surgery. However, with the development of digital technology, 3D facial scans are expected to be widely used in combination with CBCT scans or intraoral scans. The purpose of the present study was to evaluate the integration accuracy of CBCT images with facial scans obtained using a low-cost scanner.

MATERIALS AND METHODS

This study was approved by the Institutional Review Board of Chonnam National University Dental Hospital at Gwangju, Korea. Sample size calculations were performed using the G*Power program (version 3.1.9.2; Heinrich-Heine-University, Düsseldorf, Germany) with a statistical power of 80% and an alpha error of 0.05. The sample size calculations indicated a requirement of 25 patients. The sample consisted of 25 patients, 14 males and 11 females, with a mean age of 19.0 ± 11.3 years. A CBCT scan and a 3D facial scan were obtained on the same day of each patient's visit. Patients with cleft lip and palate and/or severe dentofacial deformity were excluded. CBCT scans were obtained with an Alphard Vega scanner (Asahi Roentgen, Kyoto, Japan) under the following conditions: 80 kV, 5 mA, 0.39-mm size, and 200-mm × 179-mm field of view. The CBCT scans were imported into the imaging program 3D Slicer (open-source, multiplatform, software package, version 4.11.0, http://www.slicer.org) and were segmented using threshold, islands, and scissors functions in the segment editor tab. The segmented facial model of each patient was exported as a stereolithography (STL) file format.

The 3D facial scans were obtained with the Bellus 3D facial scanner (Bellus 3D, ARC-1, Campbell, San Francisco, Calif). Using the corresponding scanner applications incorporated into the mobile device, the patient's face was scanned. Patients were instructed to position their head in a defined area on the screen until a green light showed up, indicating optimal position. During the scanning process, the scanner application showed a series of head-turning instructions on the top of the screen, together with voice instructions (Figure 1). Vibration feedback was given following the successful completion of each required head turn in accordance with the instructions. After facial scanning, the scan file was exported as an object (OBJ) file format (Figure 2).

To integrate the STL file format of the CBCT scan and OBJ file format of the facial scan, the two imaging modalities were imported into 3D reverse-engineering software (Rapidform 2006, Inus Technology, Seoul, Korea). As unnecessary areas such as hair and ears can increase the error range, the facial images were trimmed along the hair line and in front of the tragus to superimpose the two imaging modalities. Initial (global) registration was achieved through the selection of three corresponding points on the CBCT and facial scans. Subsequently, regional registration was used to finalize the registration. For regional registration, it was necessary to designate the registration area. The forehead, nasal bridge area, and malar area were included as regions of interest. Three types of measurement methods were implemented based on the region: (1) only the forehead and nasal bridge area were included as the registration area (R1), (2) the right and left malar areas were included as the registration area (R2), and (3) forehead, nasal bridge, and malar areas were included as the registration area (R3). The registration area was selected by using the function of coloring the area in the software. Registration errors were evaluated by measuring the 3D Euclidean distances between the surface points on the two surface models by using the shell/shell deviation function in the program. The average surface differences between facial scans and CBCT images were obtained using the shell/shell deviation function of the software, which calculated the closest distance between the thousands of points on the two registered surface models using an iterative closest algorithm (Figure 3).

Statistical Analysis

To evaluate the accuracy of the integration, the average surface differences between facial scans and CBCT images were calculated for each registration method, and one-way analysis of variance (ANOVA) was used to analyze the differences in the value of shell/shell deviations based on the registration area. Tukey test was used for post hoc comparisons, and statistical significance was set as .05.

RESULTS

Table 1 shows the mean and standard deviation of the shell/shell deviations, based on the three registration methods. The overall shell/shell deviations ranged

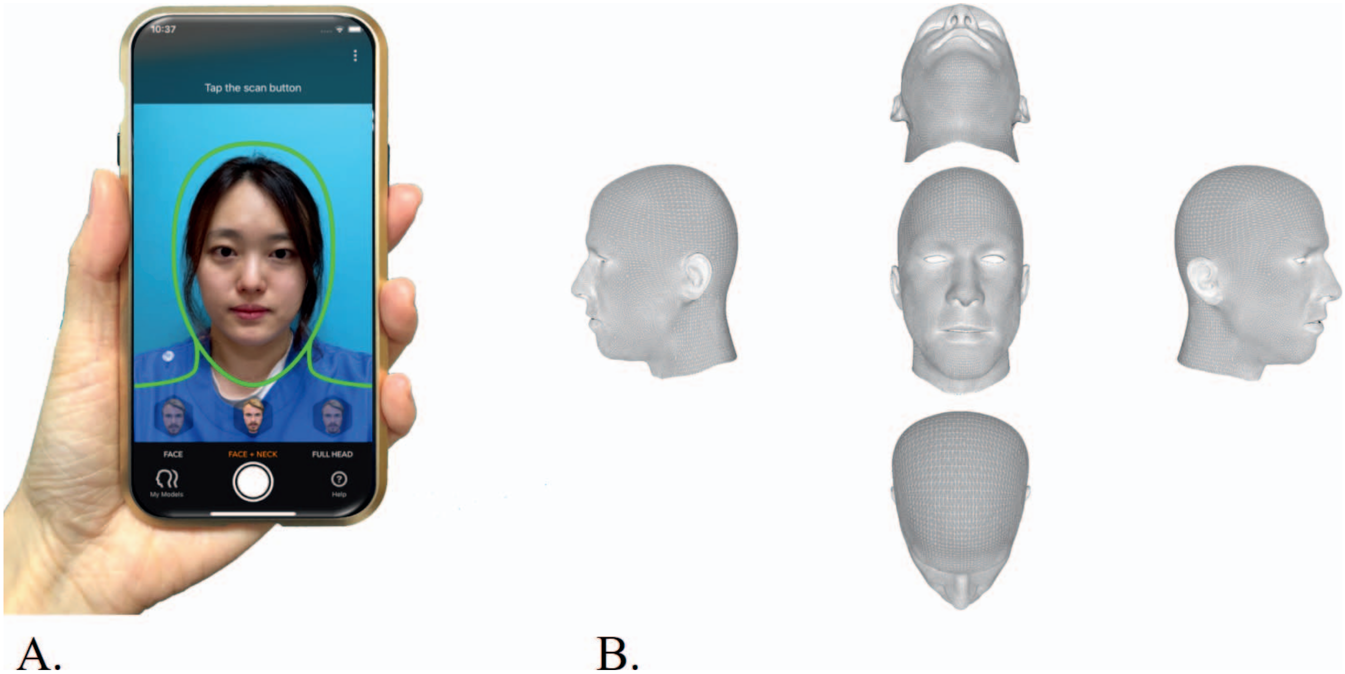

Figure 1. Facial scanner used in this study. (A) Scanning starts with the app incorporated on the mobile device. (B) Head turning required for full head scan.

from 0.77 mm to 0.93 mm. ANOVA revealed a statistically significant difference between the methods based on the registration area. The errors were greatest with the R1 method. The R3 method had significantly smaller errors than did the R1 and R2 methods. Therefore, the R3 method had the smallest error. This finding indicated that registration accuracy may be increased by including the frontal and malar areas as the registration areas (Table 1).

DISCUSSION

The objective of this study was to assess the integration accuracy of 3D facial scans obtained using a device-connected, low-cost facial scanner with CBCT images. Various 3D facial scanners have been used for facial soft-tissue evaluation in patients with facial asymmetry and in patients undergoing craniofacial surgery.[7,10] In the present study, 3D facial scans obtained using the ARC1 scanner were integrated with corresponding CBCT images, and the integration accuracy was calculated according to different registration areas. The scanner uses cameras with simultaneous localization and mapping algorithms to detect the patient's head posture and to create a 3D facial scan. The advantage of this scanner is that it is inexpensive, light, portable, and convenient to use in the clinical setting compared with other 3D facial scanning systems such as a photo-wrapping technique using a two-dimensional photo,[9] stereophotogrammetry scanning,[11–15] and structured-light scanners.

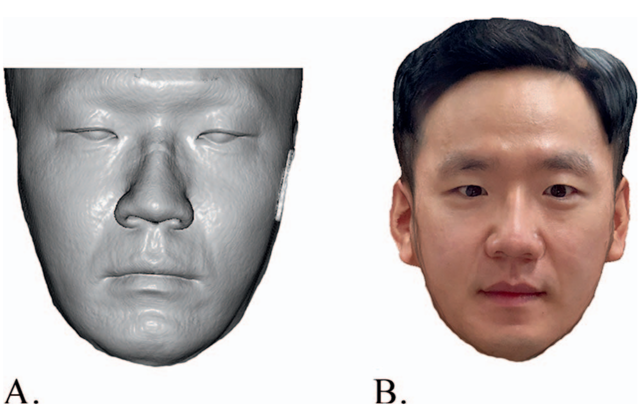

Figure 2. To integrate the facial scan into CBCT images, they were exported to the following respective file formats: (A) STL file for CBCT soft-tissue image; (B) OBJ file for facial scan.

When two data sets are compared for treatment evaluation, the images are superimposed based on the several landmarks, for example, cephalometric superimposition. However, for soft-tissue superimposition, because of the limited number of landmarks on facial soft tissue, a better technique of superimposition including surface registration (surface-based superimposition) is needed for image evaluation. The first step for surface registration is the choice of three points that can be used for initial and rough registration.[16,17] The number of points selected is not critical, because this is just for initial and rough registration; three points are recommended by the software. In addition, the

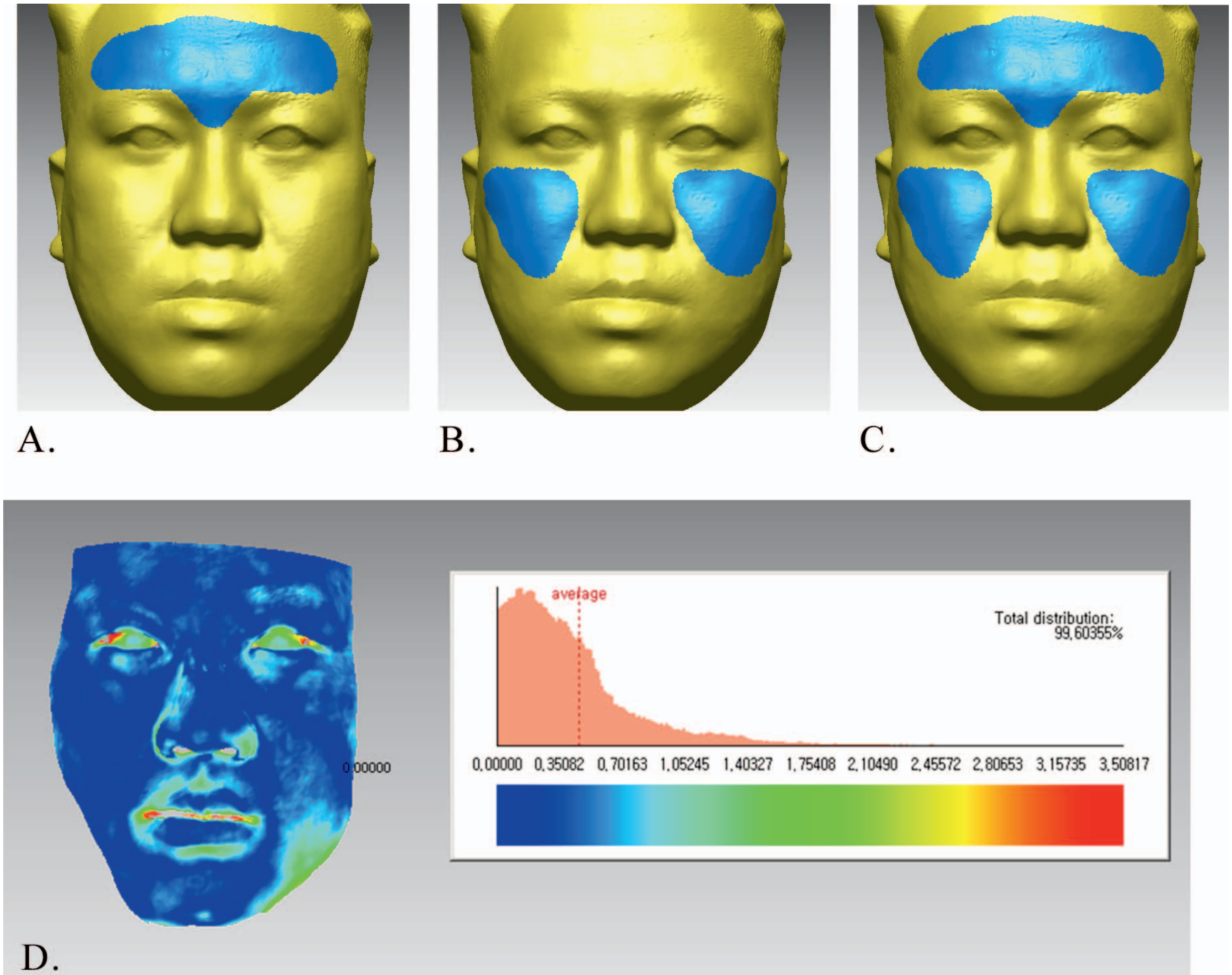

Figure 3. The blue-colored area depicts the registration area selected in each regional registration. (A) Forehead and nasal bridge only. (B) Malar area. (C) Forehead, nasal bridge, and malar areas. (D) Color-coded visualization charts show the differences between facial scans and CBCT images after the registration procedure.

threshold value was set at 1 mm in the program. Based on previous studies,[16–19] the threshold value was set at 1 mm using the program function to remove outliers. The surface registration method that uses the iterative closest-point algorithm has been proposed in previous studies.[16,17] While comparing accuracy based on the area of registration during the integration of two imaging modalities, a larger area increased accuracy, and that surface registration could also be used for an integrated image.[16,17] The registration areas used in this study were the forehead, nasal bridge area, and malar areas. In surface-based superimposition, initial registration is followed by fine regional registration for precise registration. While the initial registration is done by choosing just three points, regional registration is done based on certain regions that are stable and were not changed. Considering that the superimposition of facial soft tissue is mainly performed for treatment evaluation or postsurgical evaluation, it is logical to designate registration areas that are not related to the

Table 1. Average Surface Differences According to the Registration Areas (mm)[1]

	R1, Mean ± SD	R2, Mean ± SD	R3, Mean ± SD	*P* Value
Shell/shell deviation	0.93 ± 0.23[a]	0.89 ± 0.16[a]	0.77 ± 0.21[b]	0.001

[1] The same superscript letter indicates no statistical significance between the groups. R1, forehead and nasal bridge only; R2, malar area; R3, forehead, nasal bridge, and malar area as registration area. SD indicates standard deviation.

treatment site.[20] Based on the results, the integration of facial and CBCT scans can be performed by a surface registration protocol including the forehead, nasal bridge, and malar areas as registration areas.

Various superimposition methods can be used depending on the purpose of the evaluation. Leonardi et al.[21] used voxel-based superimposition of CBCT scans to evaluate changes in spheno-occipital synchondrosis after rapid maxillary expansion. Kim et al.[22] introduced an automated superimposition method using six landmarks on lateral cephalograms for growth evaluation. For soft-tissue evaluation, where the number of landmarks is limited, surface-based superimposition using registration areas is suitable. In addition, facial scans obtained using a low-cost device can provide clinically acceptable performance. When using such a device, chairside facial scanning can be done and patients can view their facial scans immediately, which would be helpful for patient management and favorable communication between the patient and clinician. In the near future, 3D facial scanning is expected to be used for soft-tissue analysis, including asymmetry or postsurgical swelling without CBCT.

CONCLUSIONS

- Facial scans obtained using a low-cost facial scanner showed clinically acceptable performance.
- The integration accuracy of facial and CBCT scans can be increased by including the forehead, nasal bridge, and malar regions as registration areas.

REFERENCES

1. Kau CH, Richmond S, Incrapera A, English J, Xia JJ. Three-dimensional surface acquisition systems for the study of facial morphology and their application to maxillofacial surgery. *Int J Med Robot*. 2007;3:97–110.
2. Maal TJ, van Loon B, Plooij JM, et al. Registration of 3-dimensional facial photographs for clinical use. *J Oral Maxillofac Surg*. 2010;68:2391–2401.
3. Altorkat Y, Khambay BS, McDonald JP, et al. Immediate effects of rapid maxillary expansion on the naso-maxillary facial soft tissue using 3D stereophotogrammetry. *Surgeon*. 2016;14:63–68.
4. van Loon B, Maal TJ, Plooij JM, et al. 3D stereophotogrammetric assessment of pre- and postoperative volumetric changes in the cleft lip and palate nose. *Int J Oral Maxillofac Surg*. 2010;39:534–540.
5. Petrides G, Clark JR, Low H, Lovell N, Eviston TJ. Three-dimensional scanners for soft-tissue facial assessment in clinical practice. *J Plast Reconstr Aesthet Surg*. 2021;74:605–614.
6. Gibelli D, Dolci C, Cappella A, Sforza C. Reliability of optical devices for three-dimensional facial anatomy description: a systematic review and meta-analysis. *Int J Oral Maxillofac Surg*. 2020;49:1092–1106.
7. Zhao YJ, Xiong YX, Wang Y. Three-dimensional accuracy of facial scan for facial deformities in clinics: a new evaluation method for facial scanner accuracy. *PLoS One*. 2017;5;12:e0169402.
8. Premjani P, Al-Mulla AH, Ferguson DJ. Accuracy of 3D facial models obtained from CBCT volume wrapping. *J Clin Orthod*. 2015;49:641–646.
9. Almulla S, Premjani P, Vaid NR, Fadia DF, Ferguson DJ. Evaluating the accuracy of facial models obtained from volume wrapping: 2D images on CBCT versus 3D on CBCT. *Semin Orthod*. 2018;24:443–450.
10. Modabber A, Peters F, Kniha K, et al. Evaluation of the accuracy of a mobile and a stationary system for three-dimensional facial scanning. *J Craniomaxillofac Surg*. 2016;44:1719–1724.
11. Ozsoy U, Demirel BM, Yildirim FB, Tosun O, Sarikcioglu L. Method selection in craniofacial measurements: advantages and disadvantages of 3D digitization method. *J Craniomaxillofac Surg*. 2009;37:285–290.
12. Dindaroğlu F, Kutlu P, Duran GS, Görgülü S, Aslan E. Accuracy and reliability of 3D stereophotogrammetry: a comparison to direct anthropometry and 2D photogrammetry. *Angle Orthod*. 2016;86:487–494.
13. Al-Anezi T, Khambay B, Peng MJ, O'Leary E, Ju X, Ayoub A. A new method for automatic tracking of facial landmarks in 3D motion captured images (4D). *Int J Oral Maxillofac Surg*. 2013;42:9–18.
14. Al-Anezi T, Khambay B, Peng MJ, O'Leary E, Ju X, Ayoub A. A new method for automatic tracking of facial landmarks in 3D motion captured images (4D). *Int J Oral Maxillofac Surg*. 2013;42:9–18.
15. Heike CL, Upson K, Stuhaug E, Weinberg SM. 3D digital stereophotogrammetry: a practical guide to facial image acquisition. *Head Face Med*. 2010;6:18.
16. Noh H, Nabha W, Cho JH, Hwang HS. Registration accuracy in the integration of laser-scanned dental images into maxillofacial cone-beam computed tomography images. *Am J Orthod Dentofacial Orthop*. 2011;140:585–591.
17. Sun L, Hwang HS, Lee KM. Registration area and accuracy when integrating laser-scanned and maxillofacial cone-beam computed tomography images. *Am J Orthod Dentofacial Orthop*. 2018;153:355–361.
18. Guyuron B, Ross RJ. Computer-generated model surgery: an exacting approach to complex craniomaxillofacial disharmonies. *J Craniomaxillofac Surg*. 1989;17:101–104.
19. Nkenke E, Zachow S, Benz M, et al. Fusion of computed tomography data and optical 3D images of the dentition for streak artefact correction in the simulation of orthognathic surgery. *Dentomaxillofac Radiol*. 2004;33:226–232.
20. Xiao Z, Liu Z, Gu Y. Integration of digital maxillary dental casts with 3D facial images in orthodontic patients. *Angle Orthod*. 2020;90:397–404.
21. Leonardi R, Ronsivalle V, Lagravere MO, Barbato E, Isola G, Lo Giudice A. Three-dimensional assessment of the spheno-occipital synchondrosis and clivus after tooth-borne and bone-borne rapid maxillary expansion. *Angle Orthod*. 2021;91:822–829.
22. Kim MG, Moon JH, Hwang HW, Cho SJ, Donatelli RE, Lee SJ. Evaluation of an automated superimposition method based on multiple landmarks for growing patients. *Angle Orthod*. 2022;92:226–232.